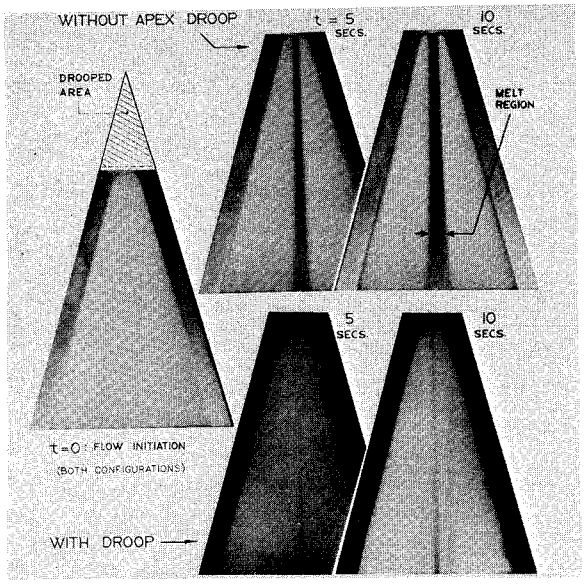


**Fig. 4 Photographs showing thermo-sensitive paint melt patterns on delta wing with and without apex droop.**

A comparison of the film records for the two-test configurations, at 5 and 10 sec (Fig. 4) shows that drooping the apex of the delta wing succeeded in greatly reducing the peak heating on the entire leeward centerline. The faint trace of vortices apparent on the droop-apex delta may result from a slight deflection of the model with wind-on, which induced a small leeward incidence at the apex. The peak heat-transfer rate associated with this weak vortex system is, however, estimated from film data to be less than one-third of the wing without droop.

Comparison with the data of Ref. 1, which showed the peak heat-transfer rate in the presence of vortices to be approximately three times the two-dimensional laminar boundary-layer calculation, suggests that the lee-surface heating on the droop-nose delta has been reduced to a level comparable with the two-dimensional laminar value. Interestingly, the spanwise variation of heat-transfer rate on a flat plate, reported in Ref. 3 and ascribed to longitudinal vortices generated within a laminar boundary layer, contain peaks similar in magnitude to those measured on the undrooped delta wing.

Together with the flow visualization studies mentioned earlier, the near-elimination of lee-meridian heating achieved by apex-drooping may be taken to favor the original conjecture that, at least at low incidence angles, the vortices arise as a result of cross flow within the laminar boundary layer.

A detailed analysis of the fluid-dynamic phenomenon in the apex region remains to be attempted; however, an intuitive approach may be taken, keeping in view the well-known two-layer model of the hypersonic laminar boundary layer,[4] consisting of a wall region of greatly reduced momentum flux and an outer layer. We consider the development of the boundary layer in a three-dimensional interaction in the region of rising pressure between the leading edge and the plane of symmtery, associated with the realinement of the inviscid streamlines initially bent inwards due to expansion of the freestream around the leading edge.[5]

The low momentum fluid, unable to penetrate the adverse pressure gradient, will be turned axially much earlier than the flow in the outer layer. This skewed boundary layer would then be expected to develop longitudinal vorticity concentrated at the junction of the two layers and in the region of the maximum pressure gradient on the wing surface. The resulting symmteric contrarotating pair of embedded vortices, much like the vortex pair following separation on delta wings, will act to drain the boundary layer away from the plane of symmtery, leading to increased shear and heat-transfer rate on the centreline.

A direct experimental confirmation of the existence of embedded vortices is desirable since they appear to be a plausible alternate mechanism to explain leeward heating peaks which until now have been exclusively related to separation vortices. The embedded vortex phenomenon, which might be common to three-dimensional boundary-layer flows on lifting bodies, appears worthy of investigation as it may hold the key to the practical problem of determining and controlling lee-side heating on hypersonic configurations.

In conclusion, it has been shown that the vortex-associated peak heating on the lee-side meridian of a delta wing at hypersonic speed can be practically eliminated by aligning the apex region with the freestream. The result suggests that the vortices are generated within the apex zone as a result of cross flow in the laminar boundary layer.

### References

[1] Whitehead, A. H., Jr., "Effect of Vortices on Delta Wing Lee-Side Heating at Mach 6," *AIAA Journal*, Vol. 8, No. 3, March 1970, pp. 599–600.

[2] Jones, R. A. and Hunt, J. L., "Use of Fusible Temperature Indicators for Obtaining Quantitative Aerodynamic Heat-Transfer Data," TR R-230, Feb. 1966, NASA.

[3] Ginoux, J. J., "Streamwise Vortices in Laminar Flow," AGARDOGRAPH 97, 1965, pp. 401–422.

[4] Stewartson, K., *Theory of Laminar Compressible Boundary Layers*, Oxford University Press, London, 1964.

[5] Fowell, L. F., "Exact and Approximate Solutions for the Supersonic Delta Wing," *Journal of the Aerospace Sciences*, Vol. 23, Aug. 1956, p. 709.

# Supersonic Nozzle Discharge Coefficients at Low Reynolds Numbers

N. M. Kuluva* and G. A. Hosack†
*Rocketdyne/North American Rockwell Corporation, Canoga Park, Calif.*

### Nomenclature

$A(\gamma)$ = function of $\gamma$ defined in Eq. (8)
$B(\gamma)$ = function of $\gamma$ defined in Eq. (9)
$C_D$ = discharge coefficient
$d_t$ = nozzle throat diameter
$f(\gamma)$ = function of $\gamma$ defined in Eq. (11)
$M$ = Mach number in the nozzle isentropic core
$Re$ = nozzle throat Reynolds number, $4\dot{W}_{ideal}/\pi d_t \mu_0$
$r$ = nozzle radius
$r_c$ = radius of curvature at the nozzle throat
$r_t$ = nozzle throat radius
$u$ = velocity in the boundary layer
$u_s$ = slip velocity at the nozzle wall
$U$ = velocity in the isentropic core
$\dot{W}_{ideal}$ = one-dimensional ideal flowrate through the nozzle
$x$ = axial coordinate along the nozzle contour
$y$ = coordinate measured normal to the nozzle contour
$\gamma$ = ratio of specific heats
$\delta$ = boundary-layer thickness
$\delta^*$ = displacement thickness
$\eta$ = dimensionless boundary-layer thickness, $y/\delta$
$\theta$ = momentum thickness
$\mu_0$ = viscosity in the nozzle stagnation chamber

Received June 9, 1970; revision received May 28, 1971. This work was supported by the Rocketdyne Physics Research and Development Program, S.A. 60681.

* Former Member of Technical Staff, Heat and Fluid Physics, Research Division.

† Member of Technical Staff, Advanced Systems, Liquid Rocket Division.

### Introduction

NOZZLES utilized for microthrustor propulsion, low density wind tunnels, and metering of small quantities of fluid often operate at low Reynolds numbers. The laminar boundary layer for many of the operating conditions becomes quite thick and causes a significant decrease in the discharge coefficient (the ratio of the actual flow through a nozzle to the ideal, one-dimensional flow).

Nozzle discharge coefficients in the region of low throat Reynolds numbers have been measured by several investigators.[1-6] Differences in the nozzle geometries produced significant differences in the measured discharge coefficients at a particular throat Reynolds number. Analytic representations have been limited either to a semiempirical description for a particular nozzle geometry[2] or to a finite difference solution of the Navier-Stokes equations in the slender channel approximation.[7]

The objective herein is to present a simple formula for calculation of the discharge coefficient in the throat Reynolds number range of 50 to $10^5$ for a wide range of nozzle geometrical configurations. The formula obtained is based on an analytic approach modified by experimentally obtained results. In the process of obtaining this formula, the nature of the boundary-layer thickness in the nozzle throat region was thoroughly investigated.

### Theoretical Approach

The discharge coefficient for flow through a nozzle may be written from the continuity equation

$$C_D = (r_t^2 - 2r_t\delta^*_t)/r_t^2 \tag{1}$$

Thus, it is only necessary to calculate the displacement thickness at the nozzle throat. The method of calculation is described below.

Because of the flow acceleration in a nozzle, the boundary-layer and momentum thickness reach their minimum values at, or quite near, the nozzle throat. This observation plus the knowledge of the axial change of Mach number in the isentropic core provides a simple means for calculating the displacement thickness. The boundary-layer equations then only need be solved algebraically at the nozzle throat to obtain the discharge coefficient. This is in contrast to the more complex solution of integrating the boundary-layer growth from some starting point upstream.

For practical calculations, the boundary-layer properties can be determined by the integral method employing a one-dimensional inviscid core and a sine-arc velocity profile in the boundary layer having the form

$$(u - u_s)/(U - u_s) = \sin(\pi\eta/2) \tag{2}$$

The density in the boundary layer is then determined for the adiabatic flow approximation, with uniform pressure across the boundary layer.

The formulation of the boundary-layer equations is based on the following assumptions: 1) The displacement thickness is a minimum at the nozzle throat. 2) Curvature effects can be neglected ($\delta/r \ll 1$). 3) Velocity slip effects at the wall can be neglected ($u_s \simeq 0$). 4) The flow is adiabatic.
The integral momentum thickness then becomes[8]

$$\frac{d\theta}{dx} = \frac{\pi}{Re}\frac{r}{\delta}\left[1 + \left(\frac{dr}{dx}\right)^2\right] - \frac{\theta}{r}\frac{dr}{dx} - \frac{1}{M}\left\{\frac{2 - M^2 + (\delta^*/\theta)}{1 + [(\gamma - 1)/2]M^2}\right\}\theta\frac{dM}{dx} \tag{3}$$

The relation between the momentum thickness and the boundary-layer thickness may be obtained by inserting Eq. (2) in the expression for the momentum thickness for compressible flow over a flat plate[9] and integrating. The result is

$$\theta = \delta\left\{\frac{2}{\pi}\left(\frac{2}{\gamma - 1}\right)^{1/2}\frac{1}{M}\tan^{-1}\left[\left(\frac{\gamma - 1}{2}\right)^{1/2}M\right] - \frac{\{1 + [(\gamma - 1)/2]M^2\}^{1/2} - 1}{[(\gamma - 1)/2]M^2}\right\} \tag{4}$$

and the relation between the displacement thickness and the boundary-layer thickness may be found in a similar manner

$$\delta^* = \delta\left\{1 - \frac{2}{\pi}\left(\frac{2}{\gamma - 1}\right)^{1/2}\frac{1}{M}\tan^{-1}\left[\left(\frac{\gamma - 1}{2}\right)^{1/2}M\right]\right\} \tag{5}$$

The wall slope, $dr/dx$, is zero at the throat for a nozzle with a continuous throat radius of curvature and the axial change of Mach number in the one-dimensional, inviscid core at the nozzle throat may be written as[10]

$$\left.\frac{dM}{dx}\right|_{M=1} = \left[\left(\frac{\gamma + 1}{2}\right)\frac{1}{r_c r_t}\right]^{1/2} \tag{6}$$

Equations (4) and (5) may be used to relate $d\theta/dx$ to $\delta^*$ and $M$. The result for the case where $d\delta^*/dx = 0$ and $M = 1$ is

$$\left.\frac{d\theta}{dx}\right|_{M=1} = \frac{\delta^*}{A(\gamma)}\left\{B(\gamma) - \left(\frac{2}{\gamma + 1}\right)^{1/2} + \left(\frac{B(\gamma) + A(\gamma) - 1}{A(\gamma)}\right) + \left(\frac{4\pi}{\gamma + 1}\right)\frac{[1 - B(\gamma)]}{A(\gamma)}\right\}\left.\frac{dM}{dx}\right|_{M=1} \tag{7}$$

where

$$A(\gamma) = 1 - \frac{2}{\pi}\left(\frac{2}{\gamma - 1}\right)^{1/2}\tan^{-1}\left(\frac{\gamma - 1}{2}\right) \tag{8}$$

and

$$B(\gamma) = \frac{[(\gamma + 1)/2]^{1/2} - 1}{(\gamma - 1)/2} \tag{9}$$

An expression for the discharge coefficient may then be obtained by setting $M = 1$ and $dr/dx = 0$ in Eqs. (3, 4, and 5) and solving Eqs. (1) and (3-7) simultaneously. The result is

$$C_D = 1 - (r_c/r_t)^{1/4}(1/Re)^{1/2}f(\gamma) \tag{10}$$

where

$$f(\gamma) = 2A(\gamma)\left\{\frac{\pi A(\gamma)}{\left(\frac{\gamma + 1}{2}\right)^{1/2}\left[A(\gamma) + B(\gamma) - 1 + \frac{2}{\pi}\left(\frac{2}{\gamma + 1}\right)^{1/2}B(\gamma)\right]}\right\}^{1/2} \tag{11}$$

or

$$f(\gamma) \simeq 0.97 + 0.86\,\gamma \tag{12}$$

### Experimental Program

An experimental program was conducted to determine the validity of the theory for calculating the discharge coefficient. Measurements were taken at the throat Reynolds numbers less than 1000. Three cases were examined: 1) a nozzle with $r_c/r_t = 2$ and argon gas, 2) a nozzle with $r_c/r_t = 20$ and argon gas, and 3) a nozzle with $r_c/r_t = 20$ and nitrogen gas. The nozzles tested were 1 mm in diameter at the throat and had conical inlet and outlet angles of 20°. The outlet expansion ratio of these nozzles was 16. A description of the test apparatus is given below.

The nozzle which exhausted into a bell jar (Fig. 1), was attached to a cylindrical tube that served as the stagnation chamber. The nozzle exhaust pressure in the bell jar was maintained between 10 and 30 $\mu$ for most of the tests by a 6 in. diffusion pump backed by a 13-cfm mechanical pump. The pressure in the stagnation chamber was monitored by

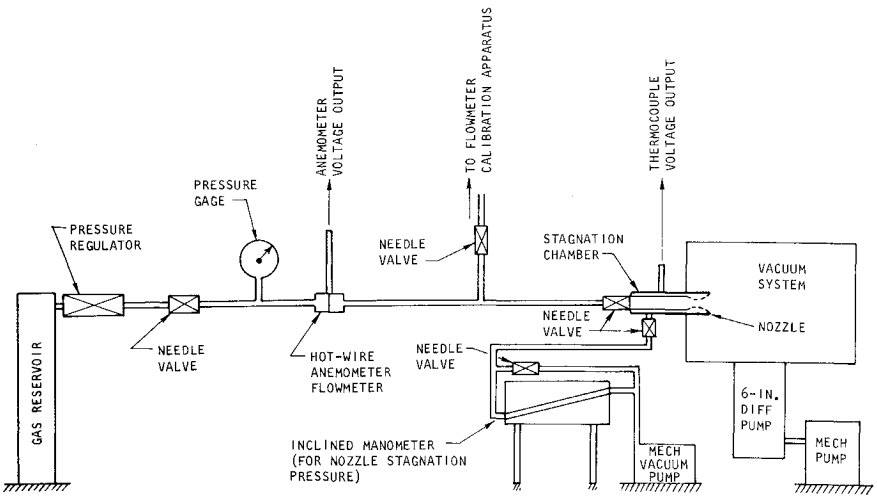


**Fig. 1 Apparatus for measuring small nozzle discharge coefficients.**

inclined manometers having scale ranges of 0 to 8 in. spread over 30-in. inclines. Meriam D-3166 indicating fluid that has a specific gravity of 1.04 and a vapor pressure of $10^{-4}$ Torr was used for pressure measurements in the nozzle throat Reynolds number range of 40 to 250; mercury was used for the manometer fluid for pressure measurements in the nozzle throat Reynolds number range of 300 to 700. In operation, one side of an inclined manometer was evacuated and the other side was used to monitor the nozzle stagnation pressure. Mass flow through the nozzle was determined by an anemometer-type probe. The probe utilized was a Thermo-Systems N35-10 mass flow sensor that had a 0.006-in. film diameter. The probe output was monitored by a digital voltmeter.

### Results and Discussion

A comparison of the theory with the experimental data is shown in Fig. 2. Good agreement was obtained for the case with argon gas and $r_c/r_t = 2$. At small values of $r_c/r_t$, the one-dimensional approximation, used to account for the change of Mach number in the inviscid core, compensates for neglecting slip and curvature effects. However, for large values of $r_c/r_t$, predicted values of the discharge coefficient using Eq. (10) were low. At large values of $r_c/r_t$, the one-dimensional approximation used to account for axial Mach number effects is more nearly correct and does not compensate for neglecting slip and curvature effects.

Although the predictions of discharge coefficient by Eq. (10) are low at large values of $r_c/r_t$, the dependence on $\gamma$ as a function of Reynolds number is seen to be valid. Consequently, Eq. (10) was extended to account for $0 \leq (r_c/r_t) \leq 20$ as explained below. The modified equation is

$$C_D = \left(\frac{r_c + 0.05\,r_t}{r_c + 0.75\,r_t}\right)^{0.019} \times \left[1 - \left(\frac{r_c + 0.10\,r_t}{r_t}\right)^{0.21} \left(\frac{1}{Re}\right)^{1/2} f(\gamma)\right] \quad (13)$$

The factor $[(r_c + 0.05\,r_t)/(r_c + 0.75\,r_t)]^{0.019}$ represents an approximation to the inviscid solution at high-throat Reynolds numbers. Its choice was motivated by a compilation of data at high Reynolds numbers[11–15] and data presented by Lefkowitz[6] for a rapidly convergent, essentially sharp-edged nozzle at low Reynolds numbers. Choice of $[(r_c + 0.10\,r_t)/r_t]^{0.21}$ was based on the data herein for $r_c/r_t = 20$.

Comparison of predictions of the discharge coefficient by Eq. (13) with experimental data of this study is shown in Fig. 3 and with the data of Smetana[2] for $r_c/r_t = 4.42$ in Fig. 4. (The throat Reynolds number used by Smetana is equal to that used in this study multiplied by $C_D$.) The agreement between theory and experiment is seen to be good over the Reynolds number range of 30 to $10^4$.

### Conclusions

Characterization of the boundary layer at a supersonic nozzle throat may be based on the assumption that the displacement thickness reaches a minimum there. The effect

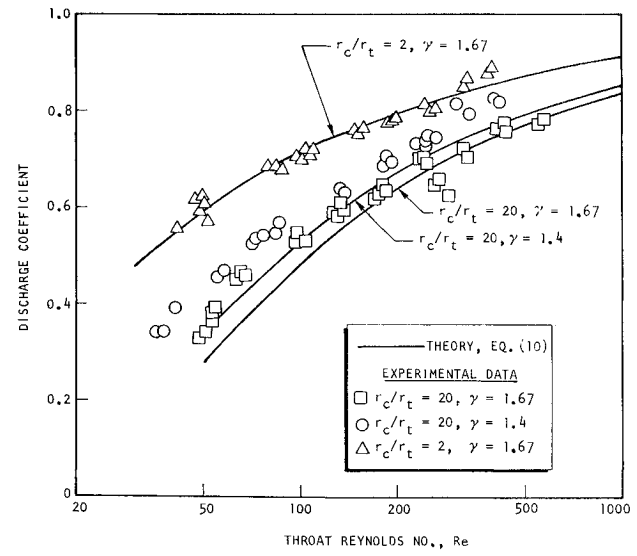


**Fig. 2 Discharge coefficient—comparison of theory [Eq. (10)] and experiment.**

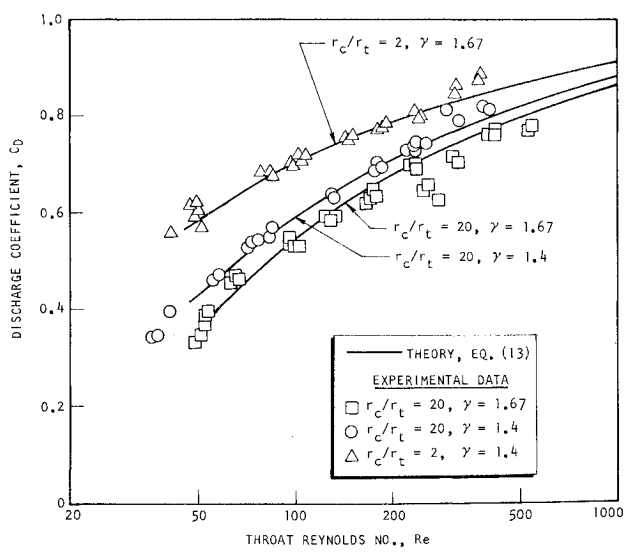


**Fig. 3 Discharge coefficient—comparison of theory [Eq. (13)] and experiment.**

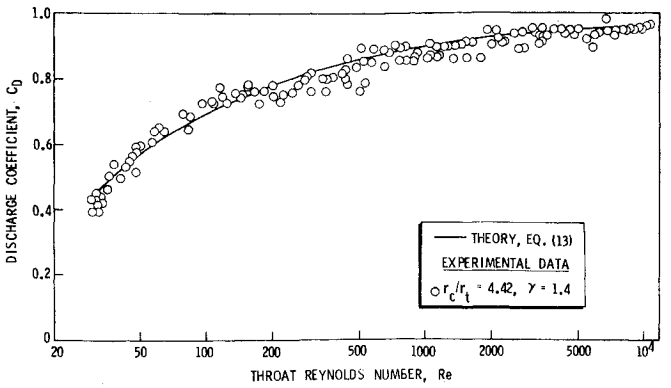


**Fig. 4 Discharge coefficient—comparison of theory [Eq. (13)] and experimental data from Ref. 2.**

of velocity slip on the discharge coefficient is significant at throat Reynolds numbers less than about $10^3$. The effect of curvature becomes important at Reynolds numbers on the order of $2 \times 10^2$.

Equation (13) is intended to be used for predicting discharge coefficients for supersonic nozzles for $0 \leq (r_c/r_t) \leq 20$ and $50 < Re < 10^5$. At throat Reynolds numbers greater than $10^5$, the boundary layer at the throat is turbulent so that the laminar theory presented in this paper is no longer applicable. At throat Reynolds numbers less than 50, the boundary layer may fill the entire throat. For the velocity and density profiles used in this study, this occurs at $C_D \simeq 0.4$ (when $u_s = 0$). When the boundary layer fills the entire throat, the flow may not necessarily choke (e.g., Fig. 1, Ref. 2) and the discharge coefficient may be strongly dependent on the back pressure. Thus, for these extremely low Reynolds numbers Eq. (13) is no longer applicable.

### References


[1] Smetana, F. O., "A Semi-empirical Description of the Discharge Characteristics of the Converging Section of a Low Density Hypersonic Nozzle," *Journal of the Aerospace Sciences*, Vol. 28, No. 12, 1961, p. 988.

[2] Smetana, F. O., "Convergent-Divergent Nozzle Discharge Characteristics in the Transition Regime Between Free Molecule and Continuum Flow," ASME Paper 63-WA-94, New York, 1963.

[3] Folsom, R. G., "Nozzle Characteristics in High Vacuum Flows—Rarefied Gas Dynamics," *ASME Transactions*, Vol. 74, 1952, p. 915.

[4] Milligan, M. W., "Nozzle Characteristics in the Transition Regime Between Continuum and Free Molecular Flow," *AIAA Journal*, Vol. 2, No. 6, June 1964, pp. 1088–1092.

[5] John, R. R., "Resistojet Research and Development—Phase II (Final Report)," NASA-CR-54688, AVSSP-0356-66-CR, Dec. 1966, Avco, Wilmington, Mass.

[6] Lefkowitz, B., "A Study of Rotational Relaxation in a Low-Density Hypersonic Freejet by Means of Impact-Pressure Measurement," Rept. 67-27, July 1967, Ph.D. dissertation, Univ. of California at Los Angeles.

[7] Rae, W. J., "Some Numerical Results on Viscous Low-Density Nozzle Flows in the Slender-Channel Approximation," AIAA Paper 69-654, San Francisco, Calif., 1969.

[8] Bartz, D. R., "Turbulent Boundary Layer Heat Transfer From Rapidly Accelerating Flow of Rocket Combustion Gases and of Heated Air," *Advances in Heat Transfer*, Vol. 2, Academic Press, New York, 1965.

[9] Schlichting, H., *Boundary Layer Theory*, 4th ed., McGraw-Hill, New York, 1960.

[10] Oswatitsch, K. and Kuerti, G., *Gas Dynamics*, Academic Press, New York, 1956.

[11] Back, L. H., Massier, P. F., and Gier, H. L., "Comparison of Measured and Predicted Flows Through Conical Supersonic Nozzle, With Emphasis on the Transonic Region," *AIAA Journal*, Vol. 3, No. 9, Sept. 1965, pp. 1606–1614.

[12] Durham, F. P. and Wood, K. D., "The Performance Characteristics of Small Rocket-Type Nozzles," Repts. 1–6, Feb. 1953–June 1955, Engineering Experiment Station, Univ. of Colorado, Boulder, Colo.

[13] "Standards for Discharge Measurement With Standardized Nozzle and Orifices," translated from *German Industrial Standard*, 1952, 4th ed., TM-952, Sept. 1940, NACA.

[14] *Fluid Meters, Their Theory and Application*, 4th edition, ASME, New York, 1937.

[15] *Flowmeter Computation Handbook*, ASME, New York, 1961.


# Sharp Slender Cones in Near-Free-Molecule Hypersonic Flow


M. I. Kussoy,* D. A. Stewart,† and C. C. Horstman‡

*Ames Research Center, NASA, Moffett Field, Calif.*


In the near-free-molecule-flow regime, only limited data drag for slender cones are currently available.[1,2] This Note presents additional drag measurements in this flow regime, obtained in air as well as helium. These results, which extend the data of Refs. 1 and 2 to higher Knudsen numbers, were obtained for cones with half angles from 2.5° to 10° at Mach numbers of 24 and 27 for air and 35 for helium. The Knudsen number based on cone diameter ($\lambda_\infty/D$) varied from 0.01 to 5.

The data were obtained in the Ames 42-Inch Shock Tunnel. The general operation and calibration procedures of this facility using a combustion driver are described elsewhere.[3,4] For completeness, a short discussion of how the freestream properties were determined for these tests will be given. The stream properties for the air tests were obtained from static and impact pressure measurements by a method[4] that assumes the air to be in equilibrium from the reservoir to an arbitrary point in the nozzle where chemical reactions and molecular vibrations are thereafter frozen.[5] At the present test conditions ($M_\infty$ = 24 and 27), static pressure measurements in the test section are unreliable because of the large corrections necessary to account for low-density effects. Therefore, the freeze Mach number for each test condition was determined using static and impact pressure measurements taken upstream in the conical nozzle where corrections for low-density effects on the static pressure probe were less than 10%. The freestream properties in the test section were then obtained using the upstream freeze Mach number, an impact pressure measurement in the test section, and a one-dimensional nozzle expansion computer program. To insure that the impact pressure measurement at the test station was free from rarefaction effects, probes of several diam. (0.5 to 4 cm) were used. The measured results indicated that these effects were negligible for probe diameters greater than 1.5 cm. The accuracy of the measured run-to-run variation of normalized dynamic pressure was ±5%; other stream properties as derived from computations of an expanding frozen flow of known active energy are estimated to be within ±10%.

With helium as a test gas the freestream properties were readily defined, because at the low reservoir enthalpy (2.4 *KJ*/gm), helium acts as a perfect gas in equilibrium. Therefore, measurements of the freestream impact pressure, reservoir total pressure, and total enthalpy completely specified the freestream properties. The accuracy of these properties, including run-to-run variation of normalized dynamic pressure, was within ±5%.

Received April 29, 1971.


* Research Scientist. Member AIAA.

† Research Scientist. Member AIAA.

‡ Research Scientist. Associate Fellow AIAA.